



ELSEVIER

Thermochimica Acta 255 (1995) 255–272

thermochimica
acta

A method of assessing solid state reactivity illustrated by thermal decomposition experiments on sodium bicarbonate

Pavan K. Heda ^a, David Dollimore ^{a,b,*}, Kenneth S. Alexander ^a,
Dun Chen ^b, Emmeline Law ^b, Paul Bicknell ^b

^a College of Pharmacy, The University of Toledo, Toledo, OH 43606, USA

^b Department of Chemistry, The University of Toledo, 2801 W. Bancroft Street, Toledo,
OH 43606, USA

Received 2 February 1994; accepted 11 October 1994

Abstract

The thermal decomposition of sodium bicarbonate (NaHCO_3) was studied under different atmospheres (dry nitrogen, air, and carbon dioxide), with various heating rates in order to characterize the substance. Various non-isothermal methods of kinetic analysis were employed in estimating the Arrhenius kinetic parameters, the activation energy and the frequency factor. All show that the most probable reaction mechanism under dry nitrogen and air is the first-order deceleratory mechanism, whereas under carbon dioxide it is the Avrami–Erofeev equation, with $n = 1.5$.

Thermogravimetric and derivative thermogravimetric analysis (TGA and DTG) were employed for comparing the solid state reactivity of different samples of sodium bicarbonate. The reaction parameters, the extent of the reaction (α) and the reaction temperature were used in comparing the reactivities of various samples of sodium bicarbonate differing in particle size and surface area produced by grinding the substance in a ball mill. A method was utilized, termed here the $\alpha_{\text{sample}} - \alpha_{\text{reference}}$ ($\alpha_s - \alpha_r$) method, by which the solid state reactivity of these samples could be compared with that of a reference. The terms α_s , α_r refer to the extent of reaction (here the extent of decomposition) at the same temperature for the sample (s) and reference (r).

Keywords: Atmosphere; Decomposition; Dentifrice; Kinetics; Mechanism; Particle size; Reactivity; Sodium bicarbonate; TA

* Corresponding author.

1. Introduction

The decomposition reaction of sodium bicarbonate is represented by the equation



in the range 100–180°C (373–453 K). The decomposition is both time and temperature dependent [1]. This decomposition process has been investigated from time to time because of its numerous uses in different types of industries [2–9]. A typical example would be its use as a dentifrice. The published information discusses the decomposition temperature and the enthalpy of the reaction. An activation energy of 85.8 kJ (20.5 kcal) has been reported for the reaction based upon the mechanism of a contracting sphere [4]. The activation energy varies with the differences in the grain size of the substance.

Grittiness is one of the historic problems which the industry has faced in formulating dental mixtures containing sodium bicarbonate. Superfine baking soda has been successfully incorporated in modern dental formulations in order to overcome this defect.

In order to assess the change in reactivity of a substance due to a change in the particle size, commercially obtained sodium bicarbonate was ground in a mill for different periods of time. The ground samples were analyzed on the TGA/DTA equipment. Commercially obtained sodium bicarbonate was used as a reference in comparing the reactivities of various samples differing in particle size and surface area.

It is recognized that this is not the same manner of affecting the crystal size as that imposed on the system by altering the actual process of crystallization. It does, however, provide an example of how reactivity can be altered by changing the “history” of the solid phase.

2. Experimental

The sodium bicarbonate used in the kinetics experiments was obtained from Fisher Chemical, Fair Lawn, New Jersey (Lot 920139). The commercial sample of sodium bicarbonate used in the grinding program was also acquired from Fisher Chemical (Lot 926222 A).

Samples of sodium bicarbonate with different particle size and surface area were produced by grinding the commercial substance in a grinding mill for different periods of time, starting from 1 h, up to 8 h.

A 4.0 g sample of sodium bicarbonate was heated in an oven at 135°C for 4 h. The residue was weighed and titrated with 0.1 N sulfuric acid. The percentage weight loss was within 0.5% of the theoretical weight loss, and the titer value matched with the value given in the literature [10] for anhydrous sodium carbonate. This confirmed the formation of sodium carbonate as the residual solid after the decomposition reaction.

The thermogravimetric and differential thermal analysis experiments were performed on an SDT 2960, simultaneous TGA/DTA unit from TA Instruments. The TGA, DTG and DTA plots were obtained for different heating rates, namely, 2, 4, 8, 12 and 16 K min⁻¹ under the atmospheres of dry nitrogen, air and carbon dioxide. The sample sizes ranged from 15 to 25 mg; the other parameters, such as the flow rate, the initial temperature, etc., remained constant. The experiments on the ground samples of sodium bicarbonate were carried out with a heating rate of 8°C min⁻¹ under an atmosphere of dry nitrogen. The sample size was 15 mg ($\pm 10\%$) for the ground samples.

The surface areas of the ground samples of sodium bicarbonate were obtained using the empirical single-point method as described by Dollimore et al. [11].

The raw data from the TA instrument was converted to DOS modality and then analyzed in the temperature range of the decomposition process.

Table 1
The common forms of $f(\alpha)$ and $G(\alpha)$ ^a

		Mechanism	$G(\alpha)$	$f(\alpha)$
Acceleratory $\alpha-t$ curve	P1	Power law	$\alpha^{1/4}$	$4\alpha^{3/4}$
			$\alpha^{1/3}$	$3\alpha^{2/3}$
			$\alpha^{1/2}$	$2\alpha^{1/2}$
			α	1
			$\alpha^{3/2}$	$2/(3\alpha^{1/2})$
			$\ln \alpha$	α
S-shaped $\alpha-t$ curve	E1	Exponential law	$(-\ln(1-\alpha))^{2/3}$	$1.5(1-\alpha)(-\ln(1-\alpha))^{1/3}$
			$(-\ln(1-\alpha))^{1/2}$	$2(1-\alpha)(-\ln(1-\alpha))^{1/2}$
			$(-\ln(1-\alpha))^{1/3}$	$3(1-\alpha)(-\ln(1-\alpha))^{2/3}$
			$(-\ln(1-\alpha))^{1/4}$	$4(1-\alpha)(-\ln(1-\alpha))^{3/4}$
			$\ln(\alpha/(1-\alpha))$	$\alpha(1-\alpha)$
			$(-\ln(1-\alpha))^2$	$0.5(1-\alpha)(-\ln(1-\alpha))^{-1}$
Deceleratory $\alpha-t$ curve	R2	Contracting surface	$(-\ln(1-\alpha))^3$	$(1/3)(1-\alpha)(-\ln(1-\alpha))^{-2}$
			$(-\ln(1-\alpha))^4$	$(1/4)(1-\alpha)(-\ln(1-\alpha))^{-3}$
			$1 - (1-\alpha)^{1/2}$	$2(1-\alpha)^{1/2}$
			$1 - (1-\alpha)^{1/3}$	$3(1-\alpha)^{2/3}$
			α^2	$1/(2\alpha)$
			$(1-\alpha) \ln(1-\alpha) + \alpha$	$-(\ln(1-\alpha))^{-1}$
			$(1 - (1-\alpha)^{1/3})^2$	$1.5(1 - (1-\alpha)^{1/3})^{-1}(1-\alpha)^{2/3}$
			$(1 - 2\alpha/3) - (1-\alpha)^{2/3}$	$1.5(1 - (1-\alpha)^{1/3})^{-1}$
			$-\ln(1-\alpha)$	$1-\alpha$
			$1/(1-\alpha)$	$(1-\alpha)^2$
			$(1/(1-\alpha))^2$	$0.5(1-\alpha)^3$
			$F3$	Third order

^a $f(\alpha)$ is the differential form and $G(\alpha)$ the integral form.

3. Theory

3.1. Kinetic analysis

The reaction rate may be described as [12]

$$d\alpha/dt = f(\alpha)k(T) \quad (2)$$

where in TGA α is a measure of the reaction extent and $\alpha = (W_i - W)/(W_i - W_f)$. Here, W is the weight or wt% of the sample at a certain time; W_i , W_f are the initial and final values for the reaction; $f(\alpha)$ is the function of α and represents the reaction mechanism, and $k(T)$ is the rate constant at a temperature T and it generally takes the Arrhenius form

$$k(T) = A \exp(-E/RT) \quad (3)$$

where A is the pre-exponential factor or frequency factor, E is the activation energy, R is the gas constant and T is the absolute temperature. Eqs. (2) and (3) combine to give

$$d\alpha/f(\alpha) = A \exp(-E/RT) dT/\beta \quad (4)$$

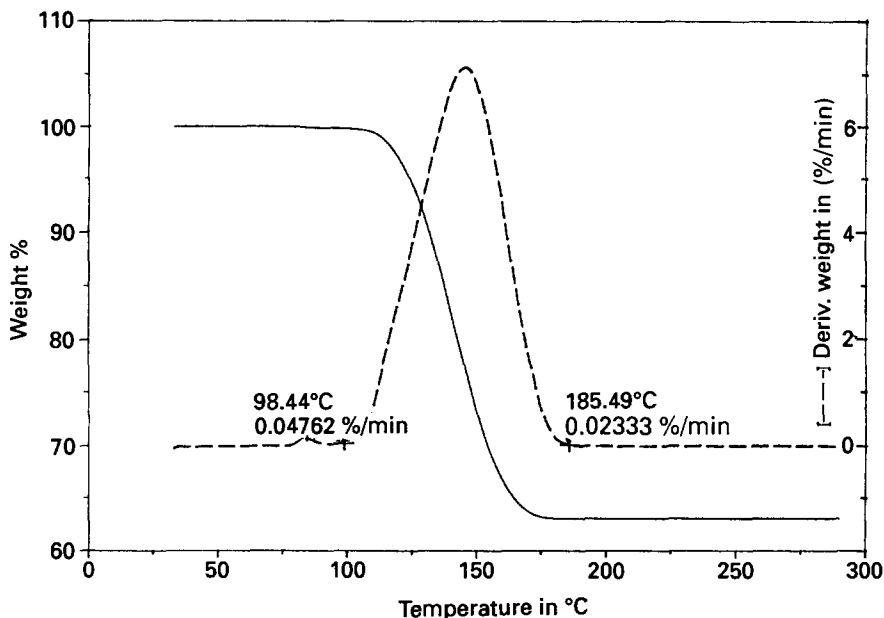


Fig. 1. The TGA and DTG curves for sodium bicarbonate at a heating rate of 8 K min^{-1} under an atmosphere of dry nitrogen.

where β is the heating rate, which is dT/dt . The integration of the right-hand side of Eq. (4) can only be approximated. The approximation proposed by Madhusudan [13] is given below and has been used in this paper.

$$\ln[G(\alpha)/T^{1.9215}] = \ln(AE/\beta R) + 3.7711 - 1.9215 \ln E - E/R \quad (5)$$

where $G(\alpha)$ is the integral form of the reaction function as given in Table 1, reproduced from Ref. [12].

3.2. Differential method

Two kinetic methods, the single-heating-rate method and the multi-heating-rate method are used in the calculation of the activation energy. In the single-heating-rate differential (SHRD) method, the logarithm of Eq. (4) is taken to give

$$\ln[(d\alpha/dt)/f(\alpha)] = \ln A - E/RT \quad (6)$$

A plot of $\ln[(d\alpha/dt)/f(\alpha)]$ vs. $1/T$ is obtained by feeding the experimental data and testing all the functions of $f(\alpha)$ from Table 1. The activation energy (E) and the frequency factor (A) can be calculated from the slope and intercept of the regression line obtained by regression analysis.

The second method was proposed by Freidman [14] and takes the form

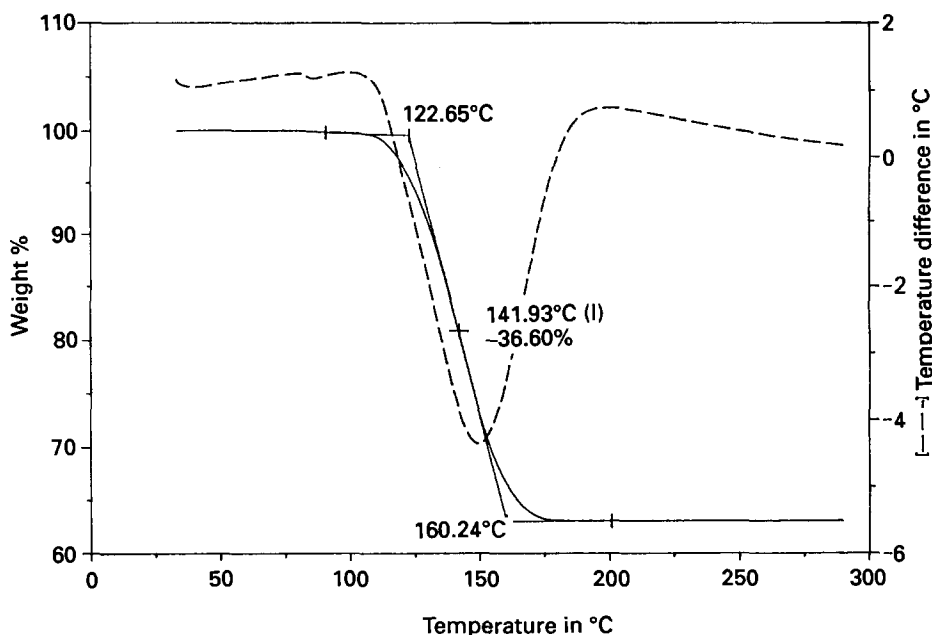


Fig. 2. The simultaneous TGA and DTA curves for sodium bicarbonate at a heating rate of 8 K min^{-1} under an atmosphere of dry nitrogen.

$$\ln(d\alpha/dt)_i = \ln Af(\alpha_i) - E/RT_i \quad (7)$$

where the subscript i refers to the value of the variable at the degree of conversion α_i from five experiments under different heating rates. Further, a plot of $\ln(d\alpha/dt)_i$ vs. $1/T_i$ is made by taking the experimental data directly from different heating-rate curves at the same α_i value; α_i takes values from 0.05 to 0.95 in steps of 0.05. The linear regression is then made to each α_i value and from the slope the activation energy E can be calculated. This method is referred to as the Freidman method.

3.3. Integral method

From Eq. (5), the plot of $\ln[G(\alpha)/T^{1.9215}]$ vs. $1/T$ is made from the single experimental heating-rate curve for all the integral forms of the function $G(\alpha)$. The activation energy E and the frequency factor A are obtained from the slope and intercept of the best fit line. This is the first integral method and is called the single-heating-rate integral (SHRI) method.

The second integral method was proposed by Ozawa [15] and takes the following form (after approximation)

$$-\log_{10}\beta_i - 0.4567E/RT_i = \text{constant} \quad (8)$$

where β_i and T_i are the heating rate and the absolute temperature for that heating rate with the same reaction extent α_i value. Five different heating rates are used. The α_i values in this paper are chosen from 0.05 to 0.95 in steps of 0.05. By plotting $\log_{10}\beta_i$ vs. $1/T_i$, the activation energy E is obtained from the slope of the best-fitting line. This method is referred to as the Ozawa method.

Solid state reactivity could be expressed in terms of these conventional kinetic parameters, but there are three terms to consider, namely the reaction rate equation, the activation energy and the pre-exponential term. A change in any one of these can cause a corresponding change in the other two. This makes comparison of the solid state reactivity difficult and a comparative method was therefore chosen for this purpose, the $\alpha_{\text{sample}} - \alpha_{\text{reference}}$ method of assessing solid state reactivity.

A thermogravimetric (TG) plot of the reference (commercial sodium bicarbonate) is obtained, and then similar TG plots are obtained on various ground samples of sodium bicarbonate using identical conditions and the same TG unit. The solid state reactivity can then be assessed from plots of $\alpha_{\text{reference}}$ (values of α , the extent

Table 2

Average activation energy results (kJ mol^{-1}) from multi-heating-rate Freidman (differential) and Ozawa (integral) methods, under different atmospheres

Experimental	Freidman method	Ozawa method
Nitrogen	87.0	98.1
Air	91.1	102.0
Carbon dioxide	93.9	119.4

of decomposition of the reference sodium bicarbonate) against the values of α for various samples (labelled as α_{sample}). The values of appropriate pairs of α_{sample} and $\alpha_{\text{reference}}$ at different temperatures $T_1, T_2, T_3, \dots, T_n$, allows an $\alpha_{\text{sample}} - \alpha_{\text{reference}}$ plot to be constructed from which the solid state reactivity may be assessed. Similarly, the solid state reactivity could be assessed from the plots obtained by choosing appropriate pairs of T_{sample} and $T_{\text{reference}}$ at different values of α .

4. Results and discussion

Fig. 1 shows the TGA and DTG curves and Fig. 2 shows the simultaneous TGA and DTA curves for sodium bicarbonate at a heating rate of 8 K min^{-1} under an atmosphere of dry nitrogen. A weight loss occurs around 373 K due to the loss of adsorbed water [10].

A 36.6% weight loss was observed for the decomposition of sodium bicarbonate, which is in close agreement to the theoretical value of 36.9%. Taking the 0.25%

Table 3

Results from the single-heating-rate differential method (SHRD) and the single-heating-rate integral method (SHRI) with respect to the first-order deceleratory mechanism ^a under dry nitrogen atmosphere for different heating rates

Heating rate/ (K m^{-1})	Parameter ^b	SHRD	SHRI
2	<i>E</i>	105.2	119.1
	<i>A</i>	9.9×10^{10}	7.9×10^{12}
	<i>R</i>	0.996	0.981
	Syx	0.113	0.294
4	<i>E</i>	100.4	117.0
	<i>A</i>	2.9×10^{10}	2.9×10^{12}
	<i>R</i>	0.995	0.983
	Syx	0.121	0.272
8	<i>E</i>	98.6	115.2
	<i>A</i>	1.6×10^{10}	8.4×10^{11}
	<i>R</i>	0.997	0.981
	Syx	0.902	0.286
12	<i>E</i>	94.3	112.3
	<i>A</i>	4.1×10^9	5.9×10^{11}
	<i>R</i>	0.951	0.989
	Syx	0.580	0.222
16	<i>E</i>	93.9	110.9
	<i>A</i>	3.5×10^9	4.7×10^{11}
	<i>R</i>	0.999	0.982
	Syx	0.055	0.279

^a $f(\alpha) = 1 - \alpha$. ^b *E*, activation energy in kJ mol^{-1} ; *A*, frequency factor in s^{-1} ; *R*, regression factor; Syx, standard error.

weight loss due to the adsorbed water [10], the remaining difference could be attributed to the impurities in the sample, the aging of the substance on the shelf and the instrumental noise.

4.1. Kinetic analysis

The activation energy can be obtained from all the methods, but it is not possible to obtain the frequency factor from the multi-heating-rate method, or by the Freidman or Ozawa methods [12]. The Freidman and Ozawa methods were used to check for the mechanism from the activation energy values. The activation energy for the same mechanism for the single-heating-rate differential method and single-heating-rate integral method was compared and the mechanism which gives the closest agreement for E was selected as the most appropriate mechanism for the decomposition process.

All the kinetic parameters were calculated using the computer programs developed by Chen et al. [16]. From the analysis it was observed that the F1 mechanism,

Table 4

Results from the single-heating-rate differential method (SHRD) and the single-heating-rate integral method (SHRI) with respect to the first-order deceleratory mechanism ^a under an atmosphere of air for different heating rates

Heating rate/ (K min ⁻¹)	Parameter ^b	SHRD	SHRI
2	E	114.4	129.7
	A	6.8×10^{11}	1.9×10^{14}
	R	0.984	0.988
	Syx	0.253	0.253
4	E	103.8	122.3
	A	7.3×10^{10}	1.9×10^{13}
	R	0.995	0.985
	Syx	0.120	0.249
8	E	97.1	116.3
	A	9.8×10^9	2.8×10^{12}
	R	0.997	0.980
	Syx	0.098	0.295
12	E	96.5	113.0
	A	7.5×10^9	9.0×10^{11}
	R	0.997	0.982
	Syx	0.090	0.282
16	E	91.7	107.5
	A	1.8×10^9	1.7×10^{11}
	R	0.998	0.982
	syx	0.070	0.277

^a $f(x) = 1 - x$. ^b E , activation energy in kJ mol⁻¹; A , frequency factor in s⁻¹; R , regression factor; Syx, standard error.

the first-order deceleratory mechanism, as given in Table 1, was the mechanism of choice, even though the A1.5 Avrami–Erofeev equation showed better regression factors under an atmosphere of carbon dioxide. The average activation energies under different atmospheres from both the multi-heating-rate differential (Freidman) and integral (Ozawa) methods are shown in Table 2. The energies of activation under an atmosphere of carbon dioxide and air were more than that observed under an atmosphere of dry nitrogen. This can be attributed to the presence of CO₂ in these atmospheres (carbon dioxide and air), which is also the gas liberated during the decomposition process, and makes it difficult for the reaction to proceed in the forward direction.

The kinetic parameters calculated from the single-heating-rate differential and integral methods, with respect to the F1 mechanism, under different atmospheres, nitrogen, air and carbon dioxide, are tabulated in Tables 3, 4 and 5 respectively. The kinetic parameters estimated with respect to the A1.5 mechanism under an atmosphere of carbon dioxide are shown in Table 6. It can be clearly seen that with

Table 5

Results from the single-heating-rate differential method (SHRD) and the single-heating-rate integral method (SHRI) with respect to the first-order deceleratory mechanism ^a under an atmosphere of CO₂ for different heating rates

Heating rate/ (K min ⁻¹)	Parameter ^b	SHRD	SHRI
2	<i>E</i>	159.0	167.4
	<i>A</i>	5.8×10^{17}	6.8×10^{18}
	<i>R</i>	0.986	0.987
	Syx	0.244	0.249
4	<i>E</i>	142.8	152.3
	<i>A</i>	4.8×10^{15}	8.7×10^{16}
	<i>R</i>	0.994	0.997
	Syx	0.152	0.074
8	<i>E</i>	128.6	146.7
	<i>A</i>	5.8×10^{13}	1.1×10^{16}
	<i>R</i>	0.998	0.988
	Syx	0.093	0.120
12	<i>E</i>	116.9	136.2
	<i>A</i>	2.0×10^{12}	4.5×10^{14}
	<i>R</i>	0.998	0.982
	Syx	0.083	0.276
16	<i>E</i>	111.2	132.3
	<i>A</i>	4.0×10^{11}	1.5×10^{14}
	<i>R</i>	0.998	0.983
	Syx	0.078	0.268

^a $f(\alpha) = 1 - \alpha$. ^b *E*, activation energy in kJ mol⁻¹; *A*, frequency factor in s⁻¹; *R*, regression factor; Syx, standard error.

Table 6

Results from the single-heating-rate differential method (SHRD) and the single-heating-rate integral method (SHRI) with respect to the Avrami–Erofeev A1.5 mechanism^a under an atmosphere of CO₂ for different heating rates

Heating rate/ (k min ⁻¹)	Parameter ^b	SHRD	SHRI
2	<i>E</i>	97.7	109.4
	<i>A</i>	6.5 × 10 ⁹	2.5 × 10 ¹¹
	<i>R</i>	0.973	0.986
	Syx	0.208	0.166
4	<i>E</i>	85.2	99.4
	<i>A</i>	2.0 × 10 ⁸	11.1 × 10 ¹⁰
	<i>R</i>	0.992	0.997
	Syx	0.102	0.049
8	<i>E</i>	76.7	95.6
	<i>A</i>	1.8 × 10 ⁷	4.2 × 10 ⁹
	<i>R</i>	0.997	0.987
	Syx	0.057	0.147
12	<i>E</i>	69.5	88.5
	<i>A</i>	2.9 × 10 ⁶	5.5 × 10 ⁸
	<i>R</i>	0.996	0.981
	Syx	0.068	0.184
16	<i>E</i>	65.0	85.9
	<i>A</i>	7.0 × 10 ⁵	2.9 × 10 ⁸
	<i>R</i>	0.996	0.982
	Syx	0.067	0.179

^a $f(\alpha) = 1.5(1-\alpha)[- \ln(1-\alpha)]^{1/3}$. ^b *E*, activation energy in kJ mol⁻¹; *A*, frequency factor in s⁻¹; *R*, regression factor; Syx, standard error.

Table 7

Summary of the results from the single-heating-rate differential method (SHRD) and the single-heating-rate integral method (SHRI) under different atmospheres with respect to different mechanism fits

Experimental atmosphere	Reaction mech. ^a	Kinetic parameter ^b	SHRD	SHRI
Nitrogen	F1	<i>E</i>	93.9–105.2	110.9–119.1
		<i>A</i>	3.5 × 10 ⁹ –2.9 × 10 ¹⁰	4.7 × 10 ¹¹ –7.9 × 10 ¹²
Air	F1	<i>E</i>	91.7–114.4	107.5–129.7
		<i>A</i>	1.8 × 10 ⁸ –6.8 × 10 ¹¹	1.7 × 10 ¹¹ –1.9 × 10 ¹⁴
Carbon dioxide	F1	<i>E</i>	111.2–159.0	132.3–167.4
Carbon dioxide	A1.5	<i>E</i>	65.0–97.7	85.9–109.4
		<i>A</i>	7.0 × 10 ⁵ –6.5 × 10 ⁹	2.9 × 10 ⁸ –2.5 × 10 ¹¹

^a F1, $f(\alpha) = 1 - \alpha$. A1.5, $f(\alpha) = 1.5(1-\alpha)[- \ln(1-\alpha)]^{1/3}$. ^b *E*, activation energy in kJ mol⁻¹; *A*, frequency factor in s⁻¹.

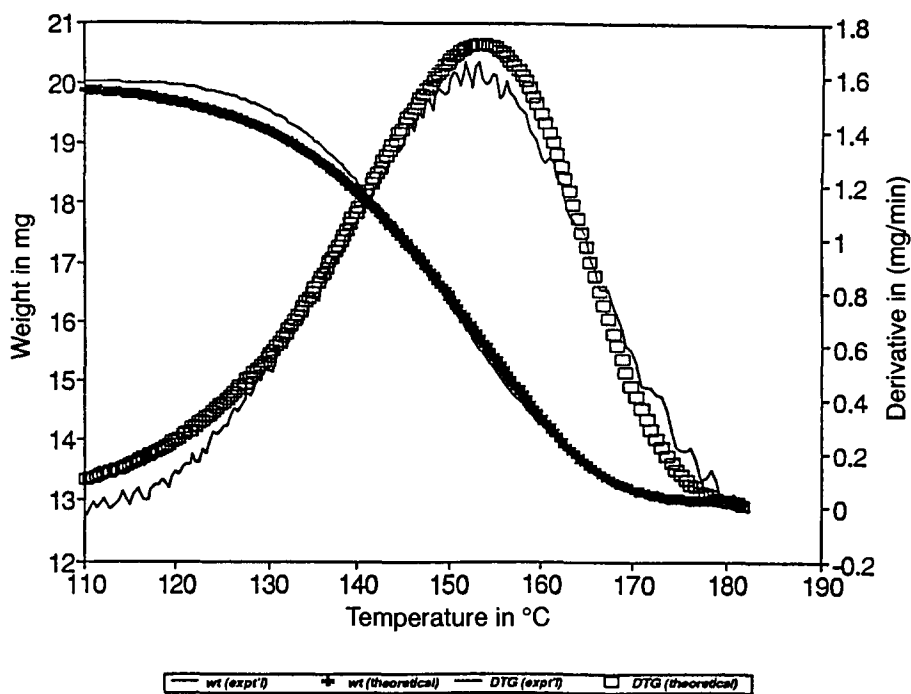


Fig. 3. The superimposed experimental and theoretical TGA and DTG curves for sodium bicarbonate at a heating rate of 16 K min^{-1} under an atmosphere of carbon dioxide, with respect to an F1 fit. Broad curves are from the theoretically simulated data.

Table 8

Results from the single-heating-rate differential method (SHRD) with respect to the first-order deceleratory mechanism, $f(\alpha) = 1 - \alpha$, for the ground samples of sodium bicarbonate under an atmosphere of dry nitrogen

Grinding time/h	Activation energy E^a / (kJ mol ⁻¹)	Frequency/factor A s ⁻¹	Regression factor R	Standard error (SE)
0 ^a	104.2	7.8×10^{10}	0.997	0.104
1	94.2	5.4×10^9	0.994	0.141
2	92.0	3.7×10^9	0.991	0.164
3	92.6	5.8×10^9	0.990	0.182
4	89.9	2.8×10^9	0.992	0.163
5	90.1	3.4×10^9	0.989	0.181
6	90.0	3.7×10^9	0.992	0.160
7	89.5	2.9×10^9	0.998	0.192
8	91.3	5.2×10^9	0.991	0.172

^a Commercially acquired sample.

Table 9

Results from the single-heating-rate integral method (SHRI) with respect to the first-order deceleratory mechanism, $G(\alpha) = -\ln(1 - \alpha)$ ^a, for the ground samples of sodium bicarbonate, under an atmosphere of dry nitrogen

Grinding time/h	Activation energy $E/$ (kJ mol ⁻¹)	Frequency factor $A/$ s ⁻¹	Regression factor R	Standard error (SE)
0 ^b	120.3	9.0×10^{12}	0.987	0.242
1	112.1	1.1×10^{12}	0.983	0.271
2	110.6	9.6×10^{11}	0.980	0.300
3	111.5	1.8×10^{12}	0.982	0.296
4	108.6	8.3×10^{11}	0.983	0.281
5	110.1	1.5×10^{12}	0.982	0.294
6	108.4	1.0×10^{12}	0.984	0.272
7	109.9	1.5×10^{12}	0.982	0.288
8	110.7	2.0×10^{12}	0.982	0.297

^a $G(\alpha)$ is the integral form of $f(\alpha)$. ^b Commercially acquired sample used as reference.

Table 10

The onset and final temperatures of reaction, the surface areas, and the ratio of the reactivity parameters for various ground samples of sodium bicarbonate

Grinding time/h	Onset temp. of the reaction/°C	Final temp. of the reaction/°C	Surface area/ (m ² g ⁻¹)	Reaction temp./°C for $\alpha = 0.5$	Reaction extent α at 140°C	α_s/α_r ^b	T_s/T_r ^b
0 ^a	99.6	180.0	6	142.6	0.443	1.000	1.000
1	95.5	178.4	14	138.2	0.550	1.242	0.969
2	92.8	175.4	22	133.9	0.650	1.467	0.934
3	90.5	172.0	31	129.9	0.750	1.693	0.911
4	89.3	170.0	35	128.1	0.780	1.761	0.898
5	88.8	167.0	40	126.1	0.817	1.844	0.884
6	87.7	166.0	43	125.0	0.841	1.898	0.877
7	87.8	166.2	43	125.4	0.831	1.876	0.879
8	87.9	166.3	43	125.5	0.821	1.876	0.880

^a Commercially acquired sample used as a reference. ^b s, sample; r, reference.

an increase in the heating rate there was a decrease in the activation energy. The activation energy also varies with the grain size of the substance. Large deviations were observed in the calculated values of the activation energy and the frequency factor under an atmosphere of CO₂. The activation energy varied from 65 to 100 kJ mol⁻¹ for the A1.5 mechanism fit and from 110 to 160 kJ mol⁻¹ with respect to F1, the first-order deceleratory mechanism fit and the single-heating-rate differential method (Table 7). Similar variation was also observed with respect to the single-heating-rate integral method (Table 7). This large variation again can be attributed

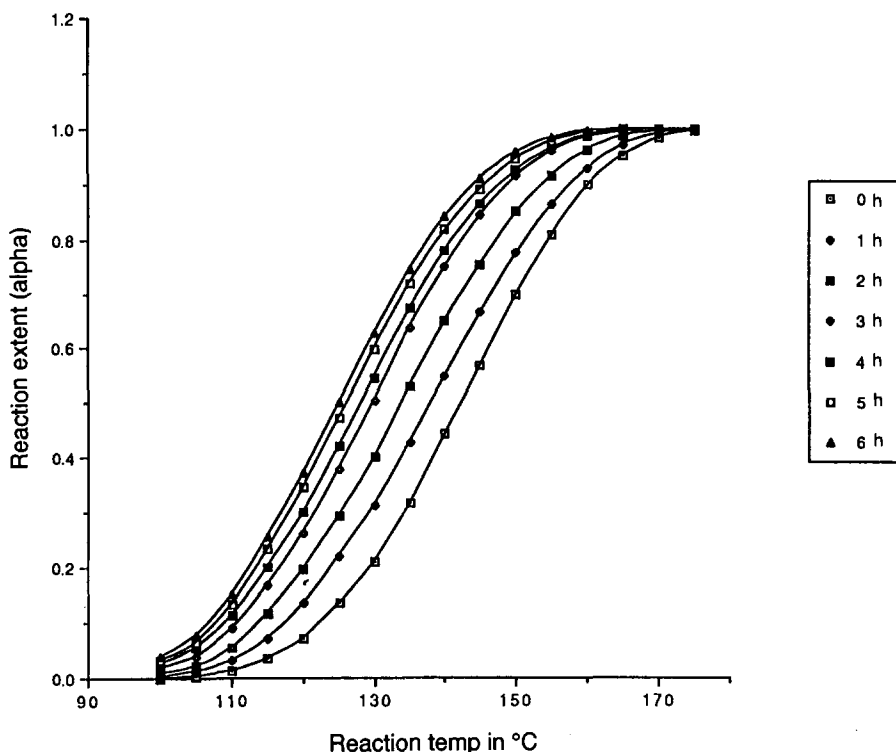


Fig. 4. Plot of α - T for the various ground samples of sodium bicarbonate as compared to that of the reference, the commercially obtained sample (0 h).

to the wide range of heating rates applied. The larger magnitude of the activation energy is due to the presence of CO_2 in these atmospheres, as already mentioned.

Fig. 3 shows that the experimental TGA and DTG curves overlap with the calculated curves for the F1 mechanism fit. A temperature lag between the theoretical and the experimental curves is ascribed to the difference in temperature recorded by the thermocouple and the actual temperature of the sample [12].

The single-heating-rate method of analysis was applied for the estimation of the kinetic parameters for the ground samples of sodium bicarbonate by ascribing a predetermined mechanism of reaction known from the prehistory of the commercially obtained reference sample. The activation energy E and the frequency factor A calculated from the single-heating-rate methods, by ascribing a predetermined F1 mechanism, $f(\alpha) = 1 - \alpha$, to the decomposition reaction, are shown in Tables 8 and 9. Even though the differences in the kinetic parameters for various samples indicate differences in the reactivities, they do not reflect the exact changes in the reactivities due to differences in the particle size or surface area. This is due to the fact that the mechanism of reaction varies with changes in the textural properties of the samples.

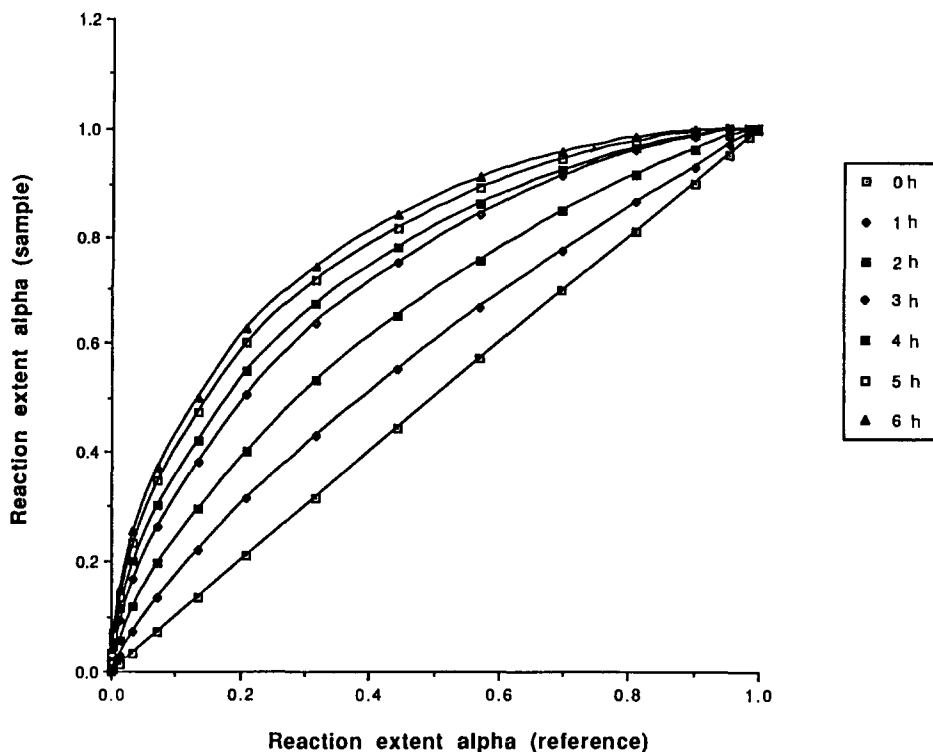


Fig. 5. Plot of $\alpha_s - \alpha_r$ for the various ground samples of sodium bicarbonate (ground up to 6 h).

4.2. Assessment of solid state reactivity

From the analysis of the ground samples on the TGA/DTA equipment, it was observed that the onset and final temperatures of the decomposition reaction decreased with an increase in the grinding time until a saturation point was reached. At this point no further reduction in particle size occurred. The onset and final temperatures of decomposition reaction for the samples of sodium bicarbonate ground for different periods of time are shown in Table 10.

An assessment of solid state reactivity is possible by use of the comparative method, (already described) and called the $\alpha_{\text{sample}} - \alpha_{\text{reference}}$ method. In this method the reactivity could be assessed by comparing a property of the sample with that of the reference. This overcomes the difficulty of comparing Arrhenius parameters where there are three interdependent terms that need to be quoted. Both reaction temperature as well as the extent of reaction were used as the parameters in comparing the reactivities of the samples with respect to the differences in their particle size and surface area.

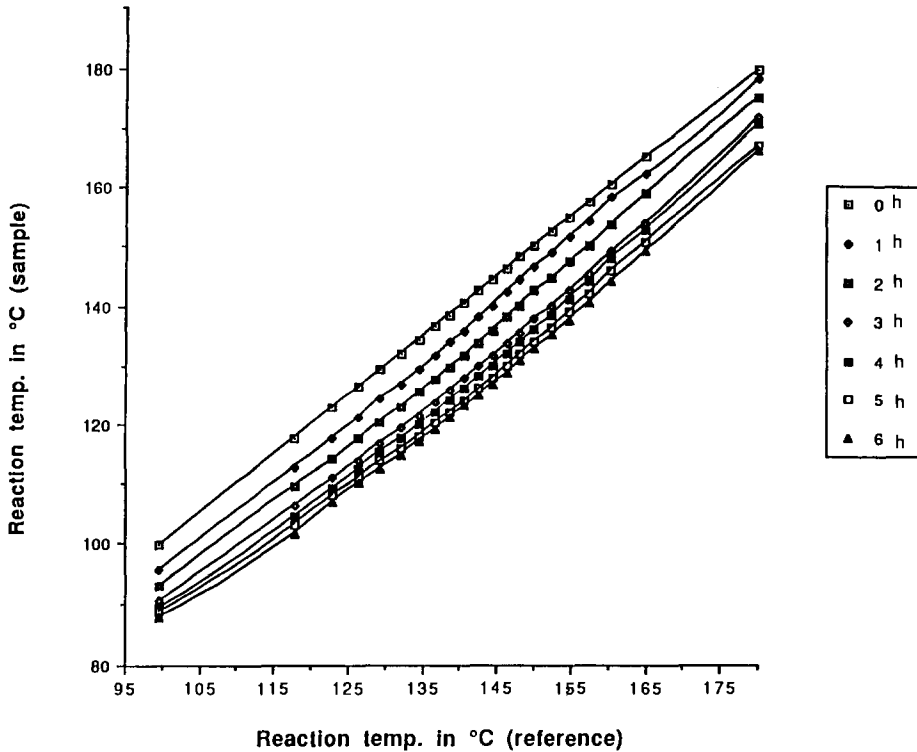


Fig. 6. Plot of $T_s - T_r$ for the various ground samples of sodium bicarbonate (ground up to 6 h).

If the solid state reactivity of the ground samples matches that of the reference sodium bicarbonate, the result will be a linear plot showing coincidence of α_{sample} and $\alpha_{\text{reference}}$ at all values of α . If the solid state reactivity of the ground samples exceeds that of the reference then the lines plotted will be on one side of the coincidence line, while if they are less than the reference sample, they will be on the other side. A similar argument can be made while comparing the other reactivity parameter, the reaction temperature. The reactivity parameters can then be compared against the surface area of the samples. The surface area for the various ground samples are tabulated in Table 10.

Fig. 4 shows the conventional method of comparing the reactivities, by plotting the extent of reaction α against the reaction temperature. Figs. 5 and 6, respectively show the behavior of the solid state reactivity of the ground samples with regard to their reaction temperatures and the extent of reaction values when compared to the reference sample, obtained commercially. The samples ground for up to six hours are compared in these figures as there was no further reduction in the particle size or change in the surface area after six hours. Figs. 7 and 8 show sintering behavior, once the saturation point is reached on grinding.

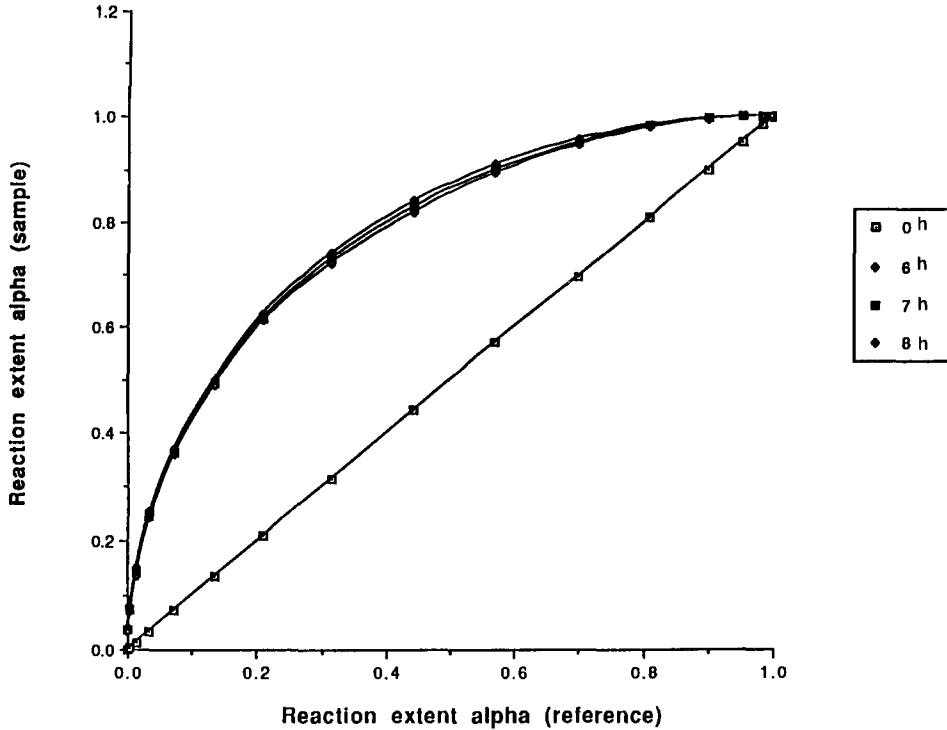


Fig. 7. Plot of $\alpha_s - \alpha_r$ for the various ground samples of sodium bicarbonate showing sintering behavior.

From Table 10 it can be seen that reactivity as expressed by α_s/α_r at 413 K or at $\alpha = 0.5$ is a function of the surface area.

5. Conclusions

The mechanism of choice for the degradation process was determined as the first-order deceleratory function, although the Avrami–Erofeev equation A1.5 showed better regression results (less variation) under an atmosphere of carbon dioxide.

In general, the activation energy decreases with an increase in the heating rate and the onset and final decomposition temperature increases with an increase in the heating rate.

Large variations were observed in the calculated values of activation energy and the frequency factor under an atmosphere of CO_2 . This large variation can be partially attributed to the wide range of heating rates employed. The larger values of the activation energy are due to the back reaction induced by decomposing the material into an atmosphere of the gaseous reaction product. A similar rationale

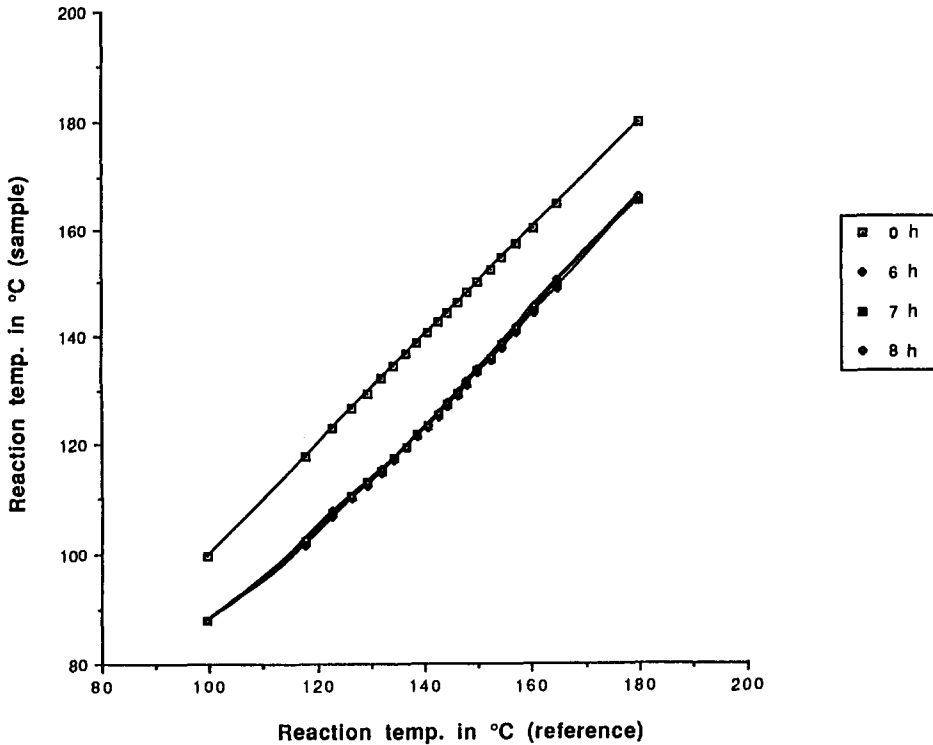


Fig. 8. Plot of $T_s - T_r$ for the various samples of sodium bicarbonate showing sintering behavior.

can be used to justify the larger values of activation energies under an atmosphere of air.

It can also be concluded that with the reduction in the particle size of sodium bicarbonate, the decomposition reaction was accelerated. Hence, a compromise has to be made between the particle size of sodium bicarbonate and its stability in the solid state when incorporated into dental formulations as a dentifrice.

The assessment of solid state reactivity by the $\alpha_{\text{sample}} - \alpha_{\text{reference}}$ plots has proved to be a reliable simple method of measuring the reactivity.

The results also show that the solid state reactivity of sodium bicarbonate is directly related to the surface area.

References

- [1] Handbook of Pharmaceutical Excipients, The American Pharmaceutical Association and The Pharmaceutical Society of Great Britain, Washington, DC, 1986.
- [2] C.V. Thomasson and D.A. Cunningham, *J. Sci. Instrum.*, 41 (1964) 308.
- [3] H.G. McAdie, *Anal. Chem.*, 35(12) (2963) 1840.
- [4] T.C. Keener, G.C. Frazier and W.T. Davis, *Chem. Eng. Commun.*, 33(1–4) (1985) 93.

- [5] R. Aleksander and M. Wesolowski, *Talanta* 27(6) (1980) 507.
- [6] E.M. Barall and L.B. Rogers, *J. Inorg. Nucl. Chem.*, 28(1) (1966) 41.
- [7] C. Duval, *Anal. Chim. Acta*, 13 (1955) 32.
- [8] T. Dupuis and C. Duval, *Chim. Anal.*, 33 (1951) 189.
- [9] P.L. Waters, *Anal. Chem.*, 32 (1960) 852.
- [10] United States Pharmacopeia, XXI edition, USP Convention Inc., Maryland, USA, 1985, p. 965.
- [11] D. Dollimore, P. Spooner and A. Turner, *Surface Technol.*, 4 (1976) 121.
- [12] D. Chen, X. Gao and D. Dollimore, *Thermochim. Acta*, 215 (1993) 65.
- [13] P.M. Madhusudanan, *Thermochim. Acta*, 97 (1986) 189.
- [14] H. Freidman, *J. Polym. Sci.*, 50 (1965) 183.
- [15] T. Ozawa, *Bull. Chem. Soc. Jpn.*, 38 (1965) 1881.
- [16] D. Chen, X. Gao and D. Dollimore, *Anal. Instrum.*, 20 (1992) 137.